European Journal of Medicinal Chemistry 45 (2010) 3169–3177

Contents lists available at ScienceDirect

European Journal of Medicinal Chemistry

journal homepage: http://www.elsevier.com/locate/ejmech

Original article

Mn(II), Co(II) and Zn(II) complexes with heterocyclic substituted thiosemicarbazones: Synthesis, characterization, X-ray crystal structures and antitumor comparison

Ming Xue Li [a], Chun Ling Chen [a], Dong Zhang [a], Jing Yang Niu [a,*], Bian Sheng Ji [b]

[a] Institute of Molecular and Crystal Engineering, College of Chemistry and Chemical Engineering, Henan University, Kaifeng 475001, P.R. China
[b] College of Pharmacy, Henan University, Kaifeng 475001, P.R. China

ARTICLE INFO

Article history:
Received 24 February 2010
Received in revised form
1 April 2010
Accepted 8 April 2010
Available online 14 April 2010

Keywords:
Thiosemicarbazone
Transition metal
Complex
Crystal structure
Cytotoxicity

ABSTRACT

Transition metal complexes $Mn(L^1)_2$ (**1**), $Mn(L^2)_2$ (**2**), $Co(L^3)_2Cl\ 4H_2O$ (**3**), $Zn(L^3)_2$ DMF (**4**), $Co(HL^4)_2(ClO_4)_2\ 3H_2O$ (**5**) and $Zn(L^5)_2$ DMF (**6**) where HL^1 = 2-acetylpyridine thiosemicarbazone, HL^2 = 2-acetylpyridine N(4)-methylthiosemicarbazone, HL^3 = 2-benzoylpyridine thiosemicarbazone, HL^4 = 2-benzoylpyridine N(4)-methylthiosemicarbazone and HL^5 = 2-benzoylpyridine N(4)-phenylthiosemicarbazone, have been synthesized. The complexes **1**, **2**, **5** and **6** were characterized by elemental analysis, IR spectra and single-crystal X-ray diffraction studies. Preliminary *in vitro* screening indicated that all the tested compounds showed significant antitumor activity against K562 leucocythemia cancer cell line.

1. Introduction

Studies related to metal-based drugs are both promising and of great interest in chemistry and biology. Heterocyclic thiosemicarbazones (TSCs) and their transition metal complexes have received considerable attention due to their coordination chemistry and broad range of pharmacological properties, notable for antiparasital, antibacterial and antitumor activities [1–6]. Triapine, a very good case in point, has been tested in phase I trial for patients with advanced solid tumors [7]. In general, thiosemicarbazones are obtained by condensation of the corresponding thiosemicarbazide with aldehydes or ketones. The biological activities of thiosemicarbazones often showed a high dependence on their substitutents. Minor modifications in the thiosemicarbazones can lead to significant change in biological activity. Earlier reports on N(4)-substituted thiosemicarbazones have concluded that the presence of a bulky group at the terminal nitrogen considerably increases biological activity [8–10]. Moreover, the metal complexes of thiosemicarbazones can exhibit bioactivities which differ from those of either ligands or the metal ions [11–13]. In some cases, the highest biological activity is associated with a metal and some side effects may decrease upon complexation [5]. Their mechanism of action is still controversial in many respects, but it is known that TSCs act by inhibiting ribonucleotide reductase, a key enzyme in the biosynthesis of DNA precursors [14].

Although thiosemicarbazones and their metal complexes derived from 2-acetylpyridine have been the subject of extensive investigation [15,16], to our knowledge there are no reports in the literature on structural and biological studies of their manganese complexes whereas manganese is an essential trace element, forming the active sites of a number of metalloproteins [17]. In addition, our previous studies on a variety of substituted thiosemicarbazones and their diverse metal complexes showed that both 2-benzoylpyridine thiosemicarbazone HL^3 and 2-benzoylpyridine N(4)-methylthiosemicarbazone HL^4 exhibited remarkable biological activity *in vitro* against K562 leukaemia cell line [18]. In particular, HL^4 inhibits K562 leukaemia cell line at concentrations more than 14,100-fold lower(0.002 μM) than HL^3(28.2 μM) only by the presence of bulky group CH_3 at position N(4) of the thiosemicarbazone moiety. On the other hand, HL^3 and its zinc complex also exhibited significant antitumor activity against lung cancer A549 cell lines [19]. Stimulated by these encouraging and promising results, it seemed useful and desirable to us to initiate systematic investigation and compare the biological activity of heterocyclic substituted thiosemicarbazones and their metal complexes.

* Corresponding author. Tel./fax: +86 378 2853650.
E-mail address: jyniu@henu.edu.cn (J.Y. Niu).

0223-5234/$ – see front matter © 2010 Elsevier Masson SAS. All rights reserved.
doi:10.1016/j.ejmech.2010.04.009

Continuing with our research program concerning the coordination and the biological properties of thiosemicarbazones [20,21], in the present work, with the main aim of comparison, we have synthesized and tested the biological activity of a series of heterocyclic substituted thiosemicarbazone ligands HL^1–HL^5 (Scheme 1) and their transition metal complexes formulated as Mn$(L^1)_2$ (**1**), Mn$(L^2)_2$ (**2**), Co$(L^3)_2$Cl $4H_2O$ (**3**), Zn$(L^3)_2$ DMF (**4**), Co$(HL^4)_2(ClO_4)_2$ $3H_2O$ (**5**) and Zn$(L^5)_2$ DMF (**6**) against K562 leukaemia cell line. Our objective is to compare the variation in antitumor activity by changing different substituted groups attached at the thiosemicarbazone moieties and metals and investigate the metal chelation effect on biological properties of the complexes. In our experiment, we have found that the title compounds with different substituents and metals show significantly different levels of antitumor activity. In addition, we also describe the synthesis, IR spectra and single crystal X-ray crystal structures of complexes **1**, **2**, **5** and **6** here.

2. Chemistry

HL^1–HL^5, **3** and **4** were prepared according to the literature method [19,20,22–26], respectively. The structures of **1**, **2**, **5** and **6** were confirmed by IR spectra and X-ray diffraction. The title compounds are all tested against K562 leukaemia cell line, with IC_{50} analysis.

The tentative assignments of the significant IR spectral bands of ligands HL^1, HL^2, HL^4, HL^5 and their complexes are presented in Table 1. The infrared spectral bands most useful for determining the mode of coordination of the ligands are the ν(C=N), ν(N–N) and ν(C=S) vibrations. The IR spectra of HL^1, HL^2, HL^4 and HL^5 do not display ν(C–SH) in the region 2500–2600 cm^{-1} indicating that in the solid state these ligands remain in the thione form [27]. The ν(C=N) band of thiosemicarbazone in four complexes undergoes a negative shift of wavenumber compared to that of the ligand, a clear sign of coordination via the imine nitrogen atom. The increase in the frequency of ν(N–N) band of the thiosemicarbazone in the spectra of complexes is due to the increase in the bond strength, again confirms the coordination via the imine nitrogen. The thioamide band, which contains considerable ν(C=S) character, is less intense in the complexes and is found at a lower frequency, suggesting coordination of the metal through sulfur. The breathing motion of the pyridine ring is shifted to a higher frequency upon complexation and is consistent with pyridine ring nitrogen coordination. The perchlorate complex **5** contains a single broad band at 1144 cm^{-1} and an unsplit band at 625 cm^{-1}, indicating the presence of ionic perchlorate [28]. Based on the above spectral evidences, it is confirmed that the thiosemicarbazone ligand is tridentate, coordinating via the imine nitrogen, the pyridyl nitrogen and thione/thiolate sulfur. These observations have also been confirmed by X-ray single crystal structure analysis.

Table 1
IR spectral assignments (cm^{-1}) of HL^1, HL^2, HL^4, HL^5, **1**, **2**, **5** and **6**.

Compound	ν(C=N)	ν(N–N)	ν(C=S)	ρ(py)
HL^1	1582	1109	835	620
1	1549	1125	798	632
HL^2	1578	1114	836	621
2	1548	1158	817	633
HL^4	1595	1144	840	625
5	1567	1171	784	648
HL^5	1594	1132	838	623
6	1538	1173	788	644

3. Results and discussion

3.1. X-ray crystallography

Table 2 summarizes crystal and refinement data for **1**, **2**, **5** and **6**. The molecular structures of **1**, **2**, **5** and **6** along with the atomic numbering scheme are shown in Figs. 1–4, respectively. Selected bond lengths and angles are listed in Table 3.

As shown in Figs. 1–4, each of complexes **1** and **2** contains the mononuclear neutral molecule composed of two identical N_2S tridentate anionic ligands wrapped around hexa-coordinated manganese (II) ion, the perchlorate complex **5** contains hexa-coordinated cobalt(II) ion with two N_2S tridentate neutral ligands, two perchlorate anions and three water solvate molecules, and the complex **6** consists of the whole mononuclear zinc(II) complex as well as one crystallization DMF molecule, respectively. For four new complexes, the thiosemicarbazone ligand as neutral ligand or in the deprotonated form coordinates in a N_2S tridentate manner with the metal atom using its imine nitrogen, thiolate (for complexes **1**, **2** and **6)** /thione(for complex **5**) sulfur and pyridyl nitrogen resulting in two 5-membered chelate rings. In view of the structural

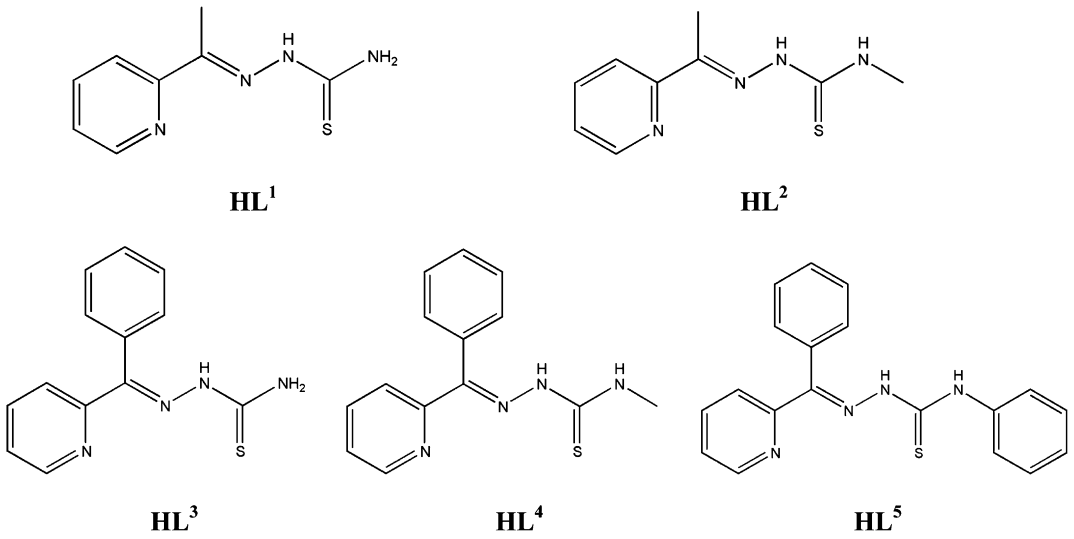

Scheme 1. Heterocyclic substituted thiosemicarbazone ligands.

Table 2
Summary of crystallographic data collection and refinement for **1**, **2**, **5** and **6**.

Crystal Data	**1**	**2**	**5**	**6**
Formula	$C_{16}H_{18}MnN_8S_2$	$C_{18}H_{22}MnN_8S_2$	$C_{28}H_{34}Cl_2CoN_8O_{11}S_2$	$C_{41}H_{37}ZnN_8S_2O$
Formula wt	441.44	469.50	852.58	801.29
Crystal system	Triclinic	Monoclinic	Monoclinic	Orthorhombic
Space group	*P-1*	$P2_1/c$	*P2(1)/n*	*Pbca*
a/Å	7.612(3)	9.50071(8)	8.6535(14)	25.711(4)
b/Å	14.962(6)	13.988(1)	32.277(5)	10.9101(15)
c/Å	17.563(8)	16.776(2)	13.479(2)	28.288(4)
α/°	74.708(8)	90.00	90.00	90.00
β/°	78.817(9)	95.512(2)	96.842(3)	90.00
γ/°	83.588(9)	90.00	90.00	90.00
Volume/Å^3	1888.9(14)	2219.1(3)	3738.1(11)	7935.1(19)
Z	4	4	4	8
ρ_{calcd}/mg m^{-3}	1.552	1.405	1.515	1.341
Crystal habit	Block	Block	Block	Block
Crystal color	Red	Red	Red	Yellow
Abs. coeff./cm^{-1}	0.939	0.804	0.780	0.769
Crystal size/mm	0.20 × 0.18× 0.16	0.36 × 0.21× 0.15	0.24 × 0.18× 0.15	0.34 × 0.25× 0.22
θ range/°	1.22–25.00	1.90–25.00	1.65–25.00	2.15–25.00
No. reflns collected	9622	9833	18862	31511
Data/restrnts/params	6529/1/487	3749/0/264	6576/0/471	6967/88/489
Gof on F^2	0.944	0.922	1.061	1.015
R_{int}	0.0653	0.0473	0.0641	0.0659
R_1, wR_2 ($I > 2\sigma(I)$)	0.0972, 0.2452	0.0446, 0.0998	0.0670, 0.1747	0.0583, 0.1664
R_1, wR_2 (all data)	0.1867, 0.2707	0.0852, 0.1081	0.0997, 0.1868	0.1103, 0.1898

similarity of these complexes, only complex **1** was described in some detail. X-ray single-crystal structure analysis reveals that the asymmetric unit of the crystal of complex **1** consists of two slightly different crystallographically independent molecules with bond lengths and angles, which agree with each other and are within normal ranges (see Table 3). The Mn(II) center is coordinated in an N_4S_2 manner by two monodeprotonated ligand moieties and form four five membered chelate rings. One sulfur atom, one imine nitrogen atom and one pyridine nitrogen atom from one ligand and one imine nitrogen atom from another ligand occupy the basal positions, the two remaining positions in the octahedral geometry are the axial ones which are occupied by one sulfur atom and one pyridine nitrogen atom from different ligands. From the bond angles, it is observed that the coordination geometry is quite far from a perfect octahedron. The dihedral angle between the two anionic ligands coordinated to Mn(1) and Mn(2) atoms was 68° and 98°, respectively.

The Mn–S distances of 2.521(3)–2.555(3) Å and Mn–N distances of 2.232(6)–2.308(6) Å agree well with those in related manganese complexes [21]. The measured C–S bond distances ca. 1.72 Å are within the normal range of C–S single bonds, indicating that the thiosemicarbazone moieties adopt the thiol tautomeric form and acted as a mononegative ligand [29]. The C–N and N–N bond lengths are intermediate between formal single and double bonds which is compatible with the notion that charge delocalization extends throughout the entire molecular skeleton, affecting the thiosemicarbazone chain as well as the ring. The two thiosemicarbazone ligands have slightly different Mn–N(pyridine) bond distances and they are longer than the Mn–N(imine) distances, this may be attributed to the fact that the imine nitrogen is a stronger base compared with the pyridine nitrogen [30].

Since the thiosemicarbazone moieties have both the hydrogen bond donors and the hydrogen bond acceptors, the species provide the possibility of forming hydrogen bonds in the crystal. The

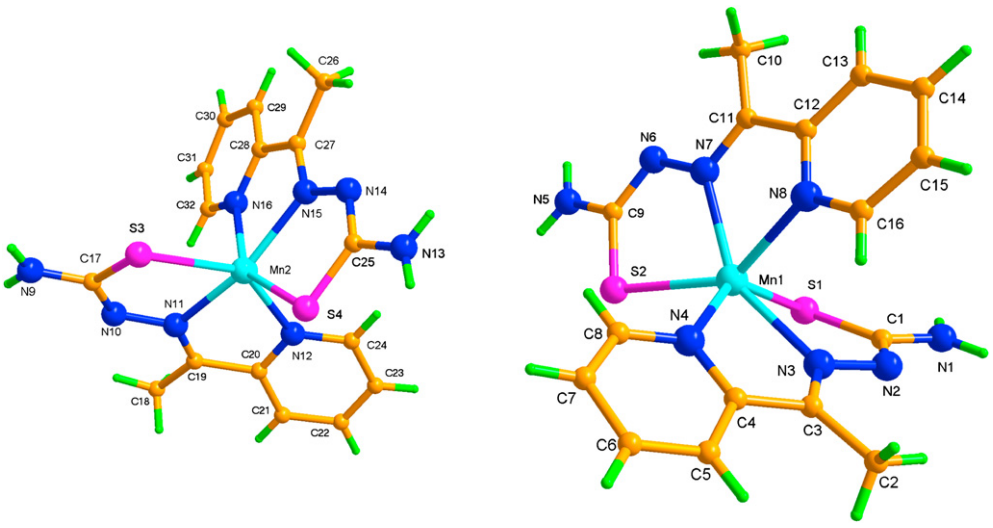

Fig. 1. Molecular structure of complex **1**.

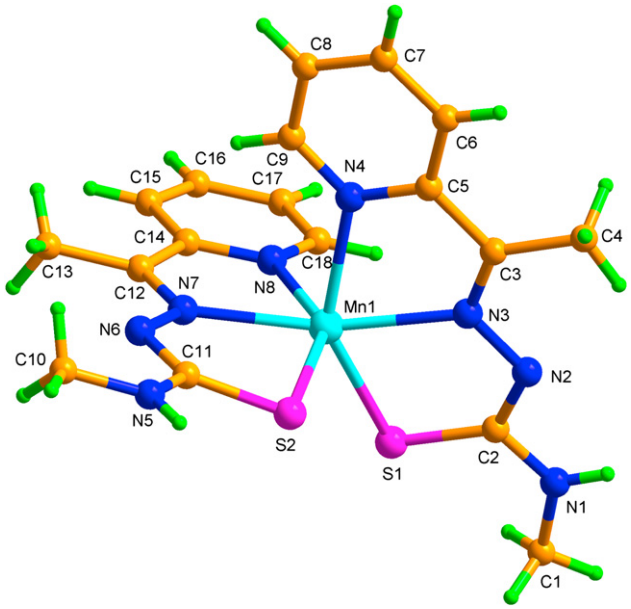

Fig. 2. Molecular structure of complex **2**.

molecules of complex **1** are held together in the crystal packing through an extended network of intermolecular hydrogen bonds involving amino nitrogen atoms N(1), N(5) and N(9), the hydrazine nitrogen atoms N(2), N(6) and N(10), the coordinated sulfur atom S(1) and S(3) (see Fig. 5, Table 4). The terminal N(1) hydrogen atom on one 2-acetylpyridine thiosemicarbazone ligand participates in forming two hydrogen bonds. One is with hydrazine nitrogen atom N(10) interaction with N(1)···N(10) 3.042(1) Å (symmetry code: $x+1, y, z+1$) and the other with the S(3) interaction with N(1)···S(3) 3.494(7) Å (symmetry code: $x, y, z+1$) from the second independent molecule. The terminal N(9) hydrogen atom also participates in forming two hydrogen bonds. One is with hydrazine nitrogen atom N(2) interaction with N(9)···N(2) 3.049(9) Å (symmetry code: $x-1, y, z-1$) and the other with the S(1) interaction with N(9)···S(1) 3.556(7) Å (symmetry code: $x, y, z-1$). In addition, the hydrazine nitrogen atom N(6) acts as H-bond acceptor while the uncoordinated terminal amino nitrogen atoms N(5) as donor. The intermolecular N(5)···N(6) separation was 3.414(1) Å with the N(5)–H(5B)···N(6) angle being about 169.3°(symmetry code: $-x+1, -y+1, -z$).

Similarily, intermolecular hydrogen bonds of complexes **2**, **5** and **6** also link the different components to stabilize the crystal structure (see Figs. 6–8), differing only in the hydrogen bond donors and acceptors (see Table 4). These intermolecular hydrogen bonds include: terminal thioamide nitrogen atoms N(1) and N(5), the hydrazine nitrogen atom N(2) , the coordinated sulfur atom S(2) for complex **2,** the terminal thioamide nitrogen N(1) and N(5), and hydrazine nitrogen N(2) and N(6) atoms of thiosemicarbazone ligands, the oxygen O(5) and O(8) atoms of perchlorate anion and the oxygen O(1w) atom of water solvent molecules for complex **5**, terminal thioamide nitrogen atoms N(1), N(5), the oxygen atom O1 from DMF solvent molecule , the coordinated sulfur atom S(2) for complex **6**, respectively.

3.2. Antitumor activity

In terms of the cytotoxic activity of thiosemicarbazones [31,32], we have tested the ability of the thiosemicarbazones and their metal complexes to inhibit tumor cell growth against K562

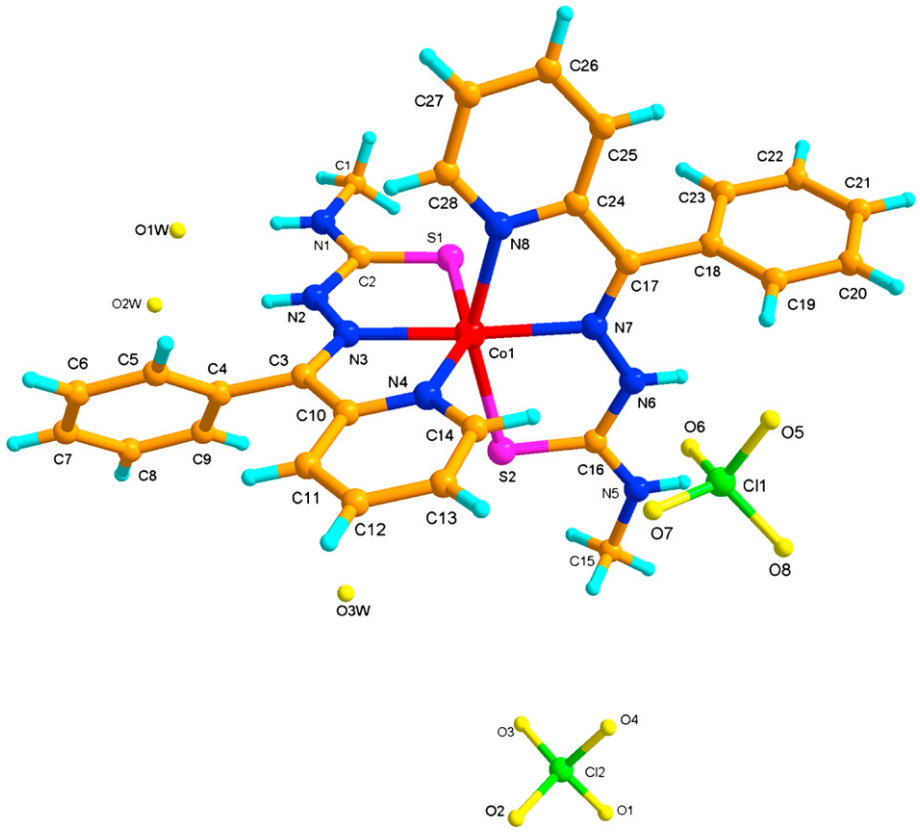

Fig. 3. Molecular structure of complex **5**.

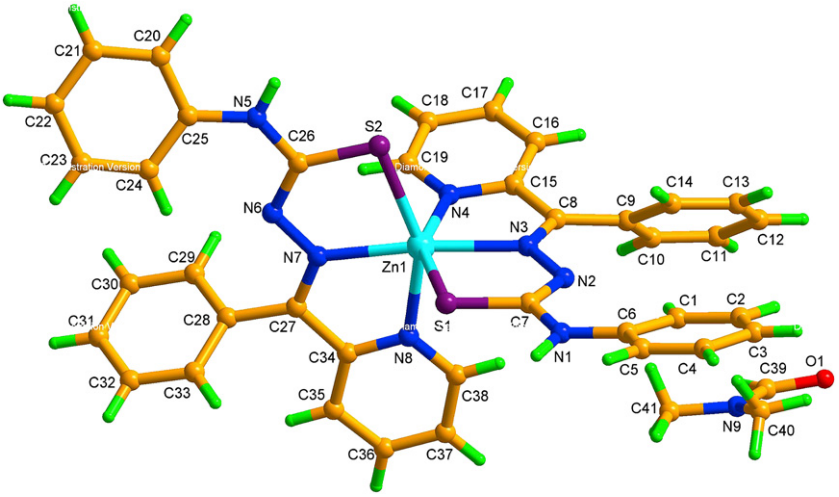

Fig. 4. Molecular structure of complex 6.

leukaemia cell line. In our experiments, IC_{50} values (compound concentration that produces 50% of cell death) in micro molar units were calculated (see Fig. 9). To comprehend the structure–activity relationship well, IC_{50} values of the parent ligands HL^3 and HL^4 were added in Fig. 9 for comparison [18]. Although a clear structure–activity relationship cannot be deduced from the limited number of compounds investigated, several preliminary conclusions may be drawn.

As shown in Fig. 9, heterocyclic substituted thiosemicarbazones and their metal complexes show particularly effective antitumor activity against K562 leukaemia cell line, due to the NNS tridentate system [33]. The comparison of cytotoxic activity of the free ligands and their metal complexes indicates that HL^2 shows much lower IC_{50} value (4.58 μM) than the HL^1 (29.74 μM), both HL^4 and HL^5 show much lower IC_{50} values (0.002 μM for HL^4, 1.43 μM for HL^5) than HL^3 (28.2 μM), complexes **2** and **5** show higher antitumor activities than complexes **1** and **3**, respectively, which indicate that these compounds showed high dependences on their substitutents that the presence of bulky groups at position N(4) of the thiosemicarbazone moiety enhanced the antitumor activities [7]. But reversed as expected where the more bulky N(4) substituent leads to more activity, N(4)-phenyl substituted thiosemicarbazone HL^5 show remarkablely lower antitumor activity than N(4)-methyl substituted thiosemicarbazone HL^4 [11]. The biochemical mechanism of cytotoxicity is not understood. In addition, HL^3 shows lower IC_{50} value (28.2 μM) than the HL^1 (29.74 μM), HL^4 shows much lower IC_{50} value (0.002 μM) than the HL^2 (4.58 μM) indicating importance of the substituent group of the parent ketone in thiosemicarbazones on antitumor activities [34,35]. And at the same time, it is clearly observed that complexation with metals has a synergetic effect on the antitumor activity of these compounds and the antitumor activity depends upon the type of metal ion. Coupling of HL^1 and HL^2 to Mn (II), respectively, leads to enhancement of the antitumor activity of Schiff base ligands. To the best of our knowledge until date, less biological information has been reported about Mn(II) complexes of thiosemicarbazones. Nevertheless, several studies have also suggested that the Mn (II) complexes have higher biological activity than their free ligands [36,37]. On the contrary, two cobalt complexes **1** and **3** show lower antitumor activities than their separate ligands, which is consistent with the previously reported cobalt cases [38,39]. As can be expected, zinc(II)complex **4** results in enhanced antitumor activity, in a similar way to that observed against lung cancer A549 cell lines [19]. This confirms the conclusion that the antitumor activities of thiosemicarbazones can be enhanced by coordinating the ligand to zinc cations [40,41]. It was surprising and not predictable that, in contrast to many zinc(II) complexes reported, complex **6** indicates

Table 3
Selected bond lengths (Å) and angles (deg) for **1**, **2**, **5** and **6**.

1		**2**		**5**		**6**	
Mn1–N3	2.286(6)	Mn1–N3	2.256(3)	Co1–N8	2.178(3)	Zn1–N7	2.174(2)
Mn1–N4	2.308(6)	Mn1–N4	2.266(3)	Co1–N7	2.157(3)	Zn1–N8	2.218(3)
Mn1–S1	2.555(3)	Mn1–S1	2.520(1)	Co1–S2	2.444(1)	Zn1–S2	2.4214(11)
Mn2–S3	2.541(3)	Mn1–N7	2.275(3)	Co1–N3	2.150(3)	Zn1–N3	2.196(3)
Mn2–N11	2.259(6)	Mn1–N8	2.270(3)	Co1–N4	2.154(3)	Zn1–N4	2.206(3)
Mn2–N12	2.265(6)	Mn1–S2	2.518(1)	Co1–S1	2.514(1)	Zn1–S1	2.4088(11)
S1–C1	1.748(8)	S1–C2	1.719(4)	S1–C2	1.676(3)	S1–C7	1.717(4)
N3–C3	1.293(9)	S2–C11	1.747(4)	S2–C16	1.688(4)	S2–C26	1.721(3)
S3–C17	1.736(8)	N3–C3	1.298(4)	N3–C3	1.288(4)	N3–C8	1.299(4)
C19–N11	1.277(9)	N7–C12	1.298(5)	N7–C17	1.290(4)	N7–C27	1.305(4)
N8–Mn1–S2	140.78(2)	N3–Mn1–S2	97.86(8)	N8–Co1–S2	153.22(8)	N7–Zn1–S1	109.25(7)
N7–Mn1–S1	96.32(2)	N8–Mn1–S2	144.83(1)	N7–Co1–S1	97.20(8)	N4–Zn1–S1	152.26(8)
N3–Mn1–S2	133.50(2)	N4–Mn1–S1	143.93(9)	N3–Co1–S2	101.84(8)	N3–Zn1–S2	111.06(8)
N4–Mn1–S1	136.67(2)	N7–Mn1–S1	123.67(8)	N4–Co1–S1	152.26(8)	N8–Zn1–S2	151.22(8)
N11–Mn2–S4	124.38(2)						
N16–Mn2–S4	146.93(2)						
N12–Mn2–S3	142.77(2)						
N15–Mn2–S3	107.04(2)						

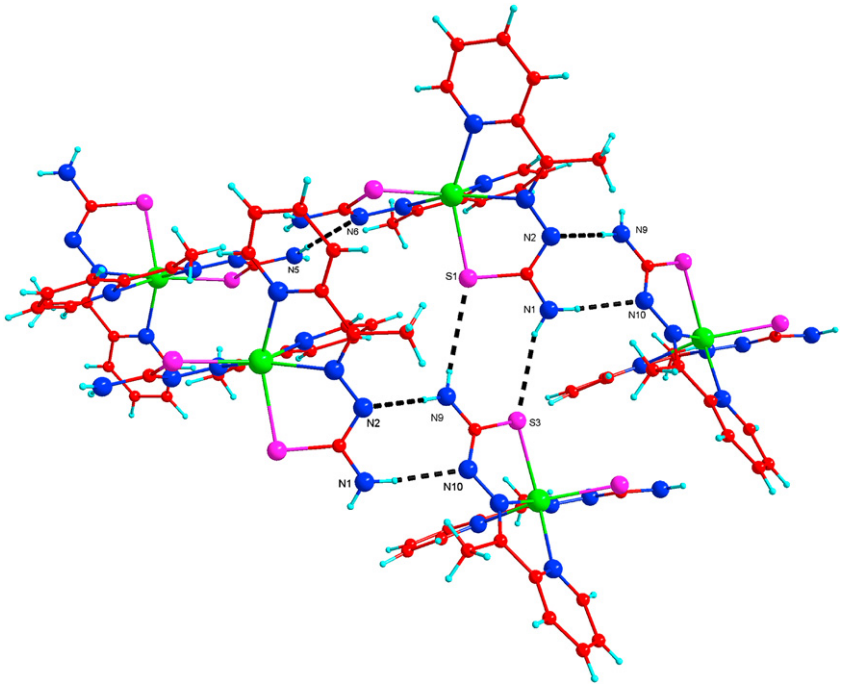

Fig. 5. Hydrogen bond in dashed lines in complex **1**.

lower cytotoxicity upon complexation similar to that of Pd complex with 2-benzoylpyridine N(4)-phenylthiosemicarbazone [11]. A detailed evaluation of mechanism will be investigated in the future. However, it should be emphasized that despite the fact that complexes **3**, **5** and **6** in this study resulted in lower antitumor activity than their respective ligands, in general their antitumor activity are still very gratifying likely attributable to striking antitumor activity of their corresponding ligands, especially HL[4]. Therefore, the complexes studied in the present work may be endowed with important antitumor activity properties and would be good candidates to be used for medical practice as a metal-based drug.

Table 4
Hydrogen bond lengths (Å) and bond angles (deg) in **1**, **2**, **5** and **6**

D–H···A	*d*(H···A)	*d*(D···A)	∠(DHA)
1			
N(1)–H(1A)–N(10)[a]	2.20	3.042(1)	166.2
(1)–H(1B)–S(3)[b]	2.68	3.494(7)	159.6
N(5)–H(5B)–N(6)[c]	2.57	3.414(1)	169.3
N(9)–H(9A)–N(2)[d]	2.19	3.049(9)	177.7
N(9)–H(9B)–S(1)[e]	2.82	3.556(7)	145.2
2			
N(1)–H(1A)–S(2)[f]	2.47	3.324(3)	171.4
N(5)–H(5A)–N(2)[g]	2.31	3.137(5)	160.7
5			
N(1)–H(1D)–O(1W)	2.09	2.867(4)	150.3
N(2)–H(2A)–O(1W)	2.15	2.843(4)	138.0
N(5)–H(5B)–O(8)[h]	2.13	2.962(5)	161.8
N(5)–H(5B)–O(5)[h]	2.43	3.170(10)	144.1
N(6)–H(6B)–O(8)[h]	2.34	3.095(5)	147.1
6			
N1–H1B–O1[i]	2.20	3.035(5)	164.9
N5–H5B–S2[j]	2.73	3.387(3)	134.6

Symmetry transformation used to generate the equivalent atoms are given in the footnotes listed below.

[a] $x+1, y, z+1$.
[b] $x, y, z+1$.
[c] $-x+1, -y+1, -z$.
[d] $x-1, y, z-1$.
[e] $x, y, z-1$.
[f] $-x+1, y-1/2, -z+1/2$.
[g] $-x+1, y+1/2, -z+1/2$.
[h] $-x+2, -y, -z+1$.
[i] $x, y+1, z$.
[j] $-x+1, -y+1, -z$.

4. Conclusions

In summary, the present investigation elucidate preliminary structure–activity relationships. The *in vitro* screening results of cytotoxic activity suggest that their mechanism of action is different and changing the different substituent groups and metal cations in the thiosemicarbazones must play a significant role in these compounds growth inhibitory activity. These promising results are encouraging further research in this field, for future applications. Our continuing and detailed studies of the toxicity of these compounds, as well as mechanism of action are in process, which could be helpful in designing more potent antitumor agents for therapeutic use.

5. Experimental

5.1. Materials and chemicals

All solvents and reagents are commercially available and were used without further purification. Instrumentation: Elemental analysis of C, H and N was performed with a Perkin-Elmer240 analyzer. The infrared spectra were recorded from KBr discs with a Nicolet 170 FT infrared spectrophotometer.

5.2. Synthesis

5.2.1. Synthesis of complex 1

An ethanol solution containing $Mn(Ac)_2 \cdot 4H_2O$ (0.12 g, 0.5 mmol) was added with constant stirring and slow heating to 30 mL of a solution of 2-acetylpyridine thiosemicarbazone (0.19 g, 1.0 mmol) in the same solvent. After refluxed for 5 h, the resultant

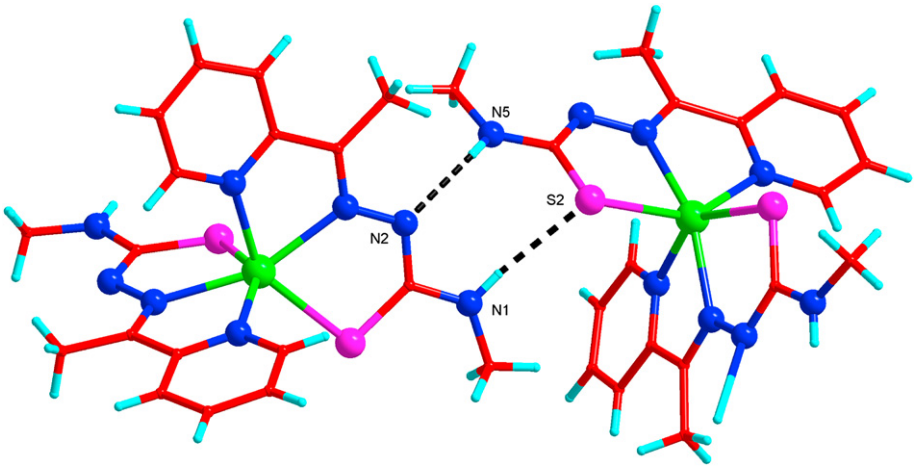

Fig. 6. Hydrogen bond in dashed lines in complex **2**.

solution was filtered. Deep-red crystals suitable for X-ray studies were obtained by slowly diffusing a layer of Et_2O into a layer of DMF solution containing **1**. Yield: 65% - $C_{16}H_{18}MnN_8S_2$ (441.44). Calc: C 43.49, H 4.08, N 25.37; found C 43.56, H 4.16, N 25.07.

*5.2.2. Synthesis of complex **2***

Complex **2** was prepared by a similar procedure to that of **1** using 2-acetylpyridine N(4)-methylthiosemicarbazone in place of 2-acetylpyridine thiosemicarbazone, the resultant solution was filtered. Deep-red crystals suitable for X-ray studies were obtained by slow evaporation of its DMF solution. Yield: 65% – $C_{18}H_{22}MnN_8S_2$ (469.50). Calc: C 46.01, H 4.69, N 23.86; found C 46.06, H 4.65, N 23.74.

*5.2.3. Synthesis of complex **5***

An ethanol solution containing $Co(ClO_4)_2 \cdot 6H_2O$ (0.091 g, 0.25 mmol) was added dropwise with constant stirring to 2-benzoylpyridine N(4)-methylthiosemicarbazone (0.135 g, 0.5 mmol) suspended in ethanol(30 mL). After refluxed for 5 h, the resultant solution was filtered. Deep-red crystals suitable for X-ray studies were obtained by slow evaporation of its ethanol solution. Yield: 60% – $C_{28}H_{34}Cl_2CoN_8O_{11}S_2$ (852.58). Calc: C 39.41, H 3.99, N 13.14; found: C 39.05, H 4.62, N 12.94.

*5.2.4. Synthesis of complex **6***

An methanol solution containing $Zn(ClO_4)_2 \cdot 6H_2O$ (0.091 g, 0.25 mmol) was added dropwise with constant stirring to 2-benzoylpyridine N(4)-phenylthiosemicarbazone (0.166 g, 0.5 mmol) suspended in methanol (30 ml). After refluxed for 5 h, the resultant solution was filtered. Yellow crystals suitable for X-ray studies were obtained by slowly diffusing a layer of Et_2O into a layer of DMF solution containing **6**. Yield: 60% – $C_{41}H_{37}ZnN_9OS_2$ (801.29). Calc: C 61.40, H 4.62, N 15.72; found: C 61.69, H 4.97, N 15.30.

5.3. X-ray crystallography

Crystallographic data were collected with a Siemens SMART-CCD diffractometer with graphite-monochromated MoK_α radiation

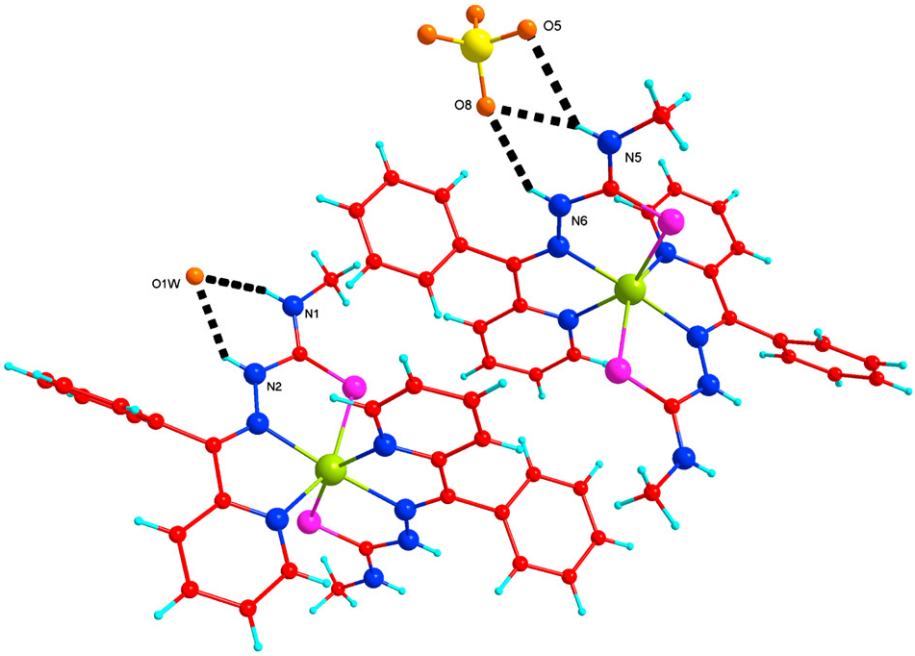

Fig. 7. Hydrogen bond in dashed lines in complex **5**.

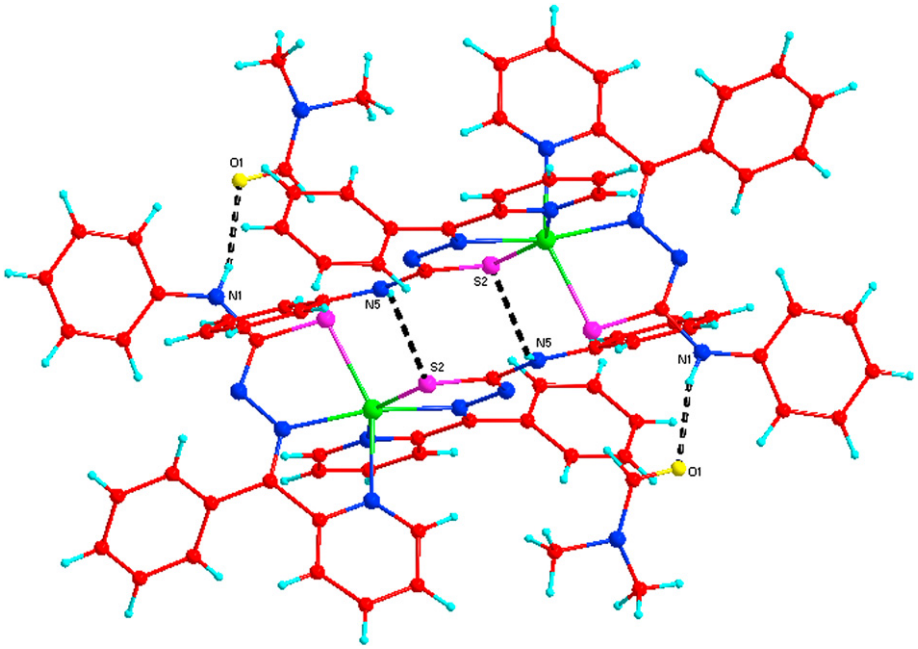

Fig. 8. Hydrogen bond in dashed lines in complex **6**.

($\lambda = 0.71073$ Å). The structure was solved by Direct Methods and refined by full-matrix least-squares on F^2 with anisotropic displacement parameters for all non-hydrogen atoms using Shelxtl [42]. Hydrogen atoms were fixed geometrically at calculated distances and allowed to ride on the parent non-hydrogen atoms, except for the hydrogen atoms of the lattice water molecules which were not added and refined in complex **5**. Crystallographic data of four complexes are summarized in Table 1.

CCDC 757299, 757300, 715337 and 757301 contain the supplementary crystallographic data for **1**, **2**, **5**, and **6**, respectively. These data can be obtained free of charge from the Cambridge Crystallographic Centre via www.ccdc.cam.ac.uk/data_request/cif.

5.4. Antitumor experiments

K562 (a human leucocythemia cancer cell line purchased from the Institute of Biochemistry and Cell Biology, SIBS, CAS) was cultured in RPMI-1640 medium supplemented with 10% FBS, 100 U mL^{-1} of penicillin, 100 μg (200 μL per well) of streptomycin at 37 °C in humid air atmosphere of 5% CO_2. Cell cytotoxicity was assessed by the MTT assay. Briefly, cells were placed into a 96-well-plate (5×10^3 cells per well). The next day the compound diluted in culture medium at various concentrations was added (200 μL per well) to the wells. 48 h later 20 μL of MTT (0.5 mg mL^{-1} MTT in PBS) was added and cells were incubated for a further 4 h. 200 μL of DMSO were added to each culture to dissolve the MTT crystals. The MTT-formazan product dissolved in DMSO was estimated by measuring absorbance at 570 nm with a micro plate reader. Then the inhibitory percentage of each compound at various concentrations was calculated, and the IC_{50} value was determined.

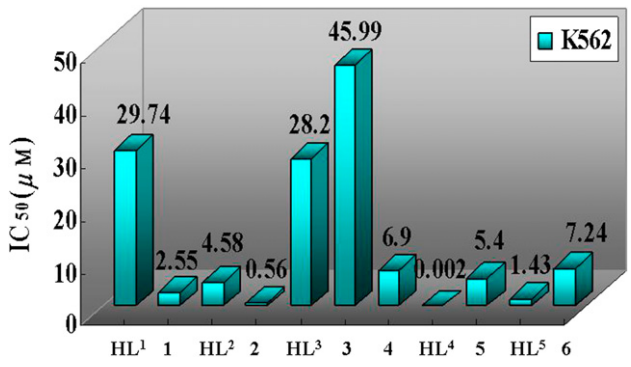

Fig. 9. The antitumor activities of HL^1–HL^5, **1**–**6** against K562 leucocythemia cell line.

Acknowledgments

This work was financially supported by the Natural Science Foundation of Henan Province(102300410093), Foundation for University Young Key Teacher by Henan Province(2009GGJS-025) and China Postdoctoral Science Foundation 20090460847.

References

[1] K.J. Duffy, A.N. Shaw, E. Delorme, S.B. Dillon, C. Erickson-Miller, L. Giampa, Y. Huang, R.M. Keenan, P. Lamb, N. Liu, S.G. Miller, A.T. Price, J. Rosen, H. Smith, K.J. Wiggall, L. Zhang, J.I. Luengo, J. Med. Chem. 45 (2002) 3573.
[2] X. Du, C. Guo, E. Hansel, P.S. Doyle, C.R. Caffrey, T.P. Holler, J.H. McKerrow, F.E. Cohen, J. Med. Chem. 45 (2002) 2695.
[3] S.A. Khan, P. Kumar, R. Joshi, P.F. Iqbal, K. Saleem, Eur. J. Med. Chem. 43 (2008) 2029.
[4] S.A. Khan, M. Yusuf, Eur. J. Med. Chem. 44 (2009) 2270.
[5] D. Kovala-Demertzi, A. Papageorgiou, L. Papathanasis, A. Alexandratos, P. Dalezis, J.R. Miller, M.A. Demertzis, Eur. J. Med. Chem. 44 (2009) 1296.
[6] I.C. Mendes, M.A. Soares, R.G. dos Santos, C. Pinheiro, H. Beraldo, Eur. J. Med. Chem. 44 (2009) 1870.
[7] W.R. Schelman, S. Morgan-Meadows, R. Marnocha, F. Lee, J. Eickhoff, W. Huang, M. Pomplun, Z.S. Jiang, D. Alberti, J.M. Kolesar, P. Ivy, G. Wilding, A.M. Traynor, Cancer Chemother. Pharmacol. 63 (2009) 1147.
[8] S.K. Jain, B.S. Garg, Y.K. Bhoon, Spectrochim. Acta A42 (1986) 959.
[9] M.E. Hossain, M.N. Alam, J. Begum, M.A. Ali, M. Nazimudhin, F.E. Smith, R.C. Hynes, Inorg. Chim. Acta. 249 (1996) 207.
[10] H. Beraldo, D. Gambino, Mini Rev. Med. Chem. 4 (2004) 159.
[11] A.P. Rebolledo, M. Vieites, D. Gambino, O.E. Piro, E.E. Castellano, C.L. Zani, E.M. Souza-Fagundes, L.R. Teixeira, A.A. Batista, H. Beraldo, J. Inorg. Biochem. 99 (2005) 698.
[12] R. Prabhakaran, S.V. Renukadevi, R. Karvembu, R. Huang, J. Mautz, G. Huttner, R. Subashkumar, K. Natarajan, Eur. J. Med. Chem. 43 (2008) 268.
[13] F.A. Beckford, M. Shaloski Jr., G. Leblanc, J. Thessing, L.C. Lewis-Alleyne, A.A. Holder, L. Li, N.P. Seeram, Dalton Trans. 10757 (2009).

[14] M.C. Miller III, C.N. Stineman, J.R. Vance, D.X. West, I.H. Hall, Anticancer Res. 18 (1998) 4131.
[15] P. Souza, A.L. Matesanz, V. Fernandez, J. Chem. Soc., Dalton Trans. (1996) 3011.
[16] N.C. Kasuga, K. Sekino, M. Ishikawa, A. Honda, M. Yokoyama, S. Nakano, N. Shimada, C. Koumo, K. Nomiya, J. Inorg. Biochem. 96 (2003) 298.
[17] A. Sreekanth, M. Joseph, H.-K. Fun, M.R.P. Kurup, Polyhedron 25 (2006) 1408.
[18] M.X. Li, C.L. Chen, C.S. Ling, J. Zhou, B.S. Ji, Y.J. Wu, J.Y. Niu, Bioorg. Med. Chem. Lett. 19 (2009) 2704.
[19] M.X. Li, J. Zhou, C.L. Chen, J.P. Wang, Z. Naturforsch. 63b (2008) 280.
[20] M.X. Li, J. Zhou, Z.L. Wang, J.P. Wang, Chinese, J. Struct. Chem. 27 (2008) 281.
[21] M.X. Li, Q.Z. Sun, Y. Bai, C.Y. Duan, B.G. Zhang, Q.J. Meng, Dalton Trans. (2006) 2572.
[22] A. Kumbhar, P. Sonawane, S. Padhye, D.X. West, R.J. Butcher, J. Chem. Cryst. 27 (1997) 533.
[23] E. Bermejo, R. Carballo, A. Castineiras, R. Dominquez, A.E. Liberta, C. Maichle-Moessmer, M.M. Salberg, D.X. West, Eur. J. Inorg. Chem. 6 (1999) 965.
[24] J.S. Casas, E.E. Castellano, J. Ellena, M.S.G. Tasende, A. Sanchez, J. Sordo, M.J. Vidarte, Inorg. Chem. 42 (2003) 2584.
[25] R.F.F. Costa, A.P. Rebolledo, T. Matencio, H.D.R. Calado, J.D. Ardisson, M.E. Cortes, B.L. Rodrigues, H. Beraldo, J. Coord. Chem. 58 (2005) 1307.
[26] D.L. Klayman, J.F. Bartosevich, T.S. Griffin, C.J. Mason, J.P. Scovill, J. Med. Chem. 22 (1979) 855.
[27] S. Singh, N. Bharti, F. Naqvi, A. Azam, Eur. J. Med. Chem. 39 (2004) 459.
[28] M. Joseph, M. Kuriakose, M.R.P. Kurup, E. Suresh, A. Kishore, S.G. Bhat, Polyhedron 25 (2006) 61.
[29] K.V. Katti, P.R. Singh, C.L. Barnes, J. Chem. Soc., Dalton Trans. (1993) 2153.
[30] A. Sreekanth, M.R.P. Kurup, Polyhedron 23 (2004) 969.
[31] R. Yanardag, T.B. Demirci, B. Ülküseven, S. Bolkent, S. Tunali, S. Bolkent, Eur. J. Med. Chem. 44 (2009) 818–826.
[32] P.F. Iqbal, A.R. Bhat, A. Azam, Eur. J. Med. Chem. 44 (2009) 2252–2259.
[33] J.G. Tojal, A.G. Orad, J.L. Serra, J.L. Pizarro, L. Lezama, M.I. Arriortua, T. Rojo, J. Inorg. Biochem. 75 (1999) 45.
[34] K. Krishnan, K. Prathiba, V. Jayaprakash, A. Basu, N. Mishra, B. Zhou, S. Hu, Y. Yen, Bioorg. Med. Chem. Lett. 18 (2008) 6248.
[35] G. Aguirre, L. Boiani, H. Cerecetto, M. Fernández, M. González, A. Denicola, L. Otero, D. Gambino, C. Rigol, C. Olea-Azar, M. Faundez, Bioorg. Med. Chem. 12 (2004) 4885.
[36] Q.X. Li, H.A. Tang, Y.Z. Li, M. Wang, L.F. Wang, C.G. Xia, J. Inorg. Biochem. 78 (2000) 167.
[37] U. El-Ayaan, M.M. Youssef, S. Al-Shihry, J. Mol. Struct. 936 (2009) 213.
[38] M. Belicchi-Ferrari, F. Bisceglie, C. Casoli, S. Durot, I. Morgenstern-Badarau, G. Pelosi, E. Pilotti, S. Pinelli, P. Tarascon, J. Med. Chem. 48 (2005) 1671.
[39] M.C. Rodríguez-Argüelles, E.C. López-Silva, J. Sanmartín, A. Bacchi, C. Pelizzi, F. Zani, Inorg. Chim. Acta 357 (2004) 2543.
[40] A. Bacchi, M. Carcelli, P. Pelagatti, C. Pelizzi, G. Pelizzi, F. Zani, J. Inorg. Biochem. 75 (1999) 123.
[41] N. Farrell, Coord. Chem. Rev. 232 (2002) 1.
[42] G.M. Sheldrick, SHELXTL (Version 5.1). Bruker AXS Inc., Madison, Wisconsin (USA), 1997.